RESEARCH ARTICLE

Influence of viscosity and impingement speed on intense hydrodynamic assist in curtain coating

J. O. Marston · M. J. H. Simmons · S. P. Decent

Abstract The onset of air entrainment for curtain coating onto a pre-wetted substrate was studied experimentally in similar parameter regimes to commercial coating [$Re = \rho \, Q/\mu = O(1)$, $We = \rho \, Q \, u_c/\sigma = O(10)$, $Ca = \mu \, U/\sigma = O(1)$]. As with coating onto dry substrates, a large flow-rate dependence was observed; termed hydrodynamic assist. The influence of the impingement speed and viscosity are shown to be critical and three qualitatively different regimes of assist are identified. The interaction of the impinging curtain with the pre-existing film also led to a significant hysteretic effect throughout the flow rate—substrate speed parameter space.

1 Introduction

High speed coating processes are central to many industries in the final stages of production of photographic films and papers, protective finishes and adhesive layers. Optimising production rates requires understanding of the mechanisms causing defects in the coating. These defects can originate at the contact line where the surface to be coated first meets the liquid which replaces the gas residing on its surface (i.e. the dynamic wetting line). Non-uniformities in the

J. O. Marston (✉) · M. J. H. Simmons
Department of Chemical Engineering,
University of Birmingham, Edgbaston,
Birmingham, UK
e-mail: jeremyom@hotmail.com

S. P. Decent
School of Mathematics, University of Birmingham,
Edgbaston, Birmingham, UK

coated layers can often be attributed to the entrainment of air bubbles at the contact line. The entrainment of air is often synonymous with dynamic wetting failure which, despite having been the focus of many studies both experimental and theoretical in nature, remains one of the few poorly understood phenomena in fluid dynamics. One particular coating method which is becoming increasingly attractive to manufacturers is curtain coating; a gravity-driven inertia-dominated method which offers a multitude of advantages over other coating techniques. One of these advantages is the ability to coat at high speeds, typically of the order of 1,000 m/min, which is attributed to the inertial pressure load of the falling curtain suppressing the entrainment of air at the contact line. This feature of curtain coating was termed ''hydrodynamic assist'' by Blake et al. (1994) and has since been examined for a number of curtain and jet coating geometries (Blake et al. 1999, 2004; Yamamura et al. 1999, 2006; Clarke 2002; Marston et al. 2006a, b).

One noticeable feature of all of the above mentioned studies (in certain regions of the operating parameter space) is a switch in behaviour and the violation of the usual inverse viscosity dependence of the maximum coating speed, an observation well documented in the literature (Benkreira 2004).

This switch to higher coating speeds for increasing viscosity is observed once critical conditions are reached; Clarke (2002) reported the switch onto rough surfaces above a critical surface roughness. Blake et al. (2004) observed higher coating speeds than previously reported by using a high liquid viscosity at increased curtain heights onto smooth dry surfaces. Yamamura et al. (1999) and Marston et al. (2006a, b) both observed the switch with increasing viscosity of a New-

tonian liquid coating a pre-wetted substrate. The physical mechanism for the switch to higher coating speeds for increasing viscosity, as with the mechanism of dynamic wetting failure, is not yet fully understood.

In this paper, new experimental results are presented for a curtain coating geometry where the surface is pre-wetted with the coating liquid. By studying the effect of viscosity and curtain impingement speed, we show a switch to different assist regimes above critical conditions, identifying three distinct, increasingly intense modes of hydrodynamic assist.

In addition to the usual experimental approach to the air entrainment problem, i.e. fixing all experimental parameters and increasing the substrate speed only (horizontal examination), the air entrainment boundary was approached by fixing substrate speeds and altering the flow rate through the curtain (vertical examination), see Marston et al. (2006a) for full details of this approach. By manual clearing of instability, secondary critical speeds for the onset of instability are identified. This new approach shows that large regions of the parameter space are no longer completely stable or unstable, but metastable.

2 Experimental

The experimental setup shown schematically in Fig. 1 has been detailed previously (see Marston et al. 2006a). A polished stainless steel wheel is continuously rotated and scraped with squeegee blades to provide a uniformly pre-wetted surface with a typical film thickness of $O(10^{-6})$m. The curtain originates from a four-slot die, fed from a precision gear pump accurate to within 3.5%. The width of the curtain (90 mm) was maintained using wire or Perspex edge guides, without
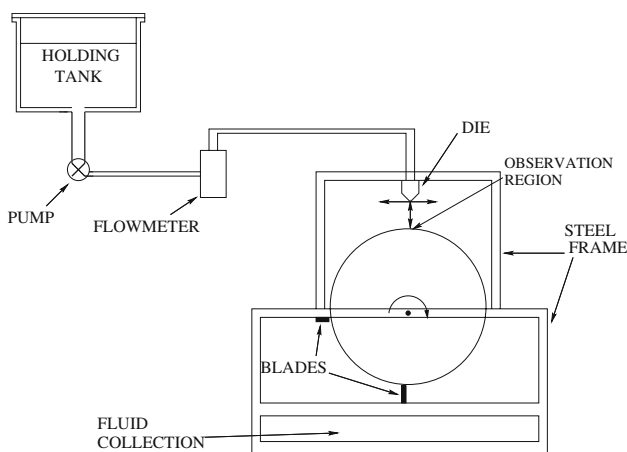

Fig. 1 Experimental apparatus

the need for an edge flush. The curtain height was varied by means of a screw thread in the range 10.7 cm $\leq h \leq$ 17.7 cm, resulting in corresponding impingement speeds 1.4 m s^{-1} $\leq u_c \leq$ 1.86 m s^{-1} and curtain widths (at the impingement zone) 55 μm $\leq w \leq$ 715 μm (based on the entire range of flow rates 1 cm^2 s^{-1} $\leq Q \leq$ 10 cm^2 s^{-1}). The coating liquids used were Newtonian aqueous solutions of glycerol of varying concentrations to produce viscosities in the range 0.028 Pa s $\leq \mu \leq$ 0.878 Pa s. Although the range here is restricted to 0.097 Pa s $\leq \mu \leq$ 0.213 Pa s, which exhibits all the qualitative features. The resulting dimensionless parameters are of the following order; $Re = \rho\ Q/\mu = O(1)$, $We = \rho\ Q\ u_c/\sigma = O(10)$, $Ca = \mu\ U/\sigma = O(1)$ where ρ, μ and σ are the density, dynamic viscosity and surface tension of the liquid, respectively. Resulting pressure loads at the base of the curtain are within the range 2.6 kPa $\leq \rho\ u_c^2 \leq$ 4.4 kPa.

Measurements of the wheel speed at the onset of instability, defined by air entrainment, gross failure or heel with recirculation (discussed in detail later), were made for a number of solutions of varying viscosity over the range of curtain heights to produce coating windows. The onset of instability was determined by first fixing the curtain flow rate, Q, and then increasing the substrate speed, U ("horizontal" analysis). Instability was also examined by first fixing U and then increasing Q ("vertical" analysis). Hysteresis was examined by determining the clearance of instability by reducing either Q or U, respectively. All observations of the onset and clearance of instability were made with the naked eye. All data points were repeated at least three times and observed variation was less than 3%. By increasing the curtain height and/or liquid viscosity above critical values, we identify three qualitatively distinct modes of hydrodynamic assist.

3 Results and discussion

Figure 2 shows a series of air entrainment curves for a low viscosity (μ = 0.097 Pa.s) glycerol solution for increasing curtain heights (h = 10.7, 15.2 and 17.7 cm). The curves were produced by setting Q and increasing U and are typical of coating windows observed using a curtain geometry (Blake et al. 1994, 2004). The main features are the increasing maximum coating speeds U_{max} = 1.46, 1.81 and 2.11 m s^{-1} at flow rates Q_{max} = 1.88, 1.79 and 1.66 cm^2 s^{-1} with increasing curtain heights and the convergence of all three curves to a single substrate speed at which the onset of instability is no longer influenced by the flow field, $U_i \sim$ 0.6 m s^{-1}, at a flow rate $Q_i \gtrsim$ 5 cm^2 s^{-1}. U_{max} is clearly depen-
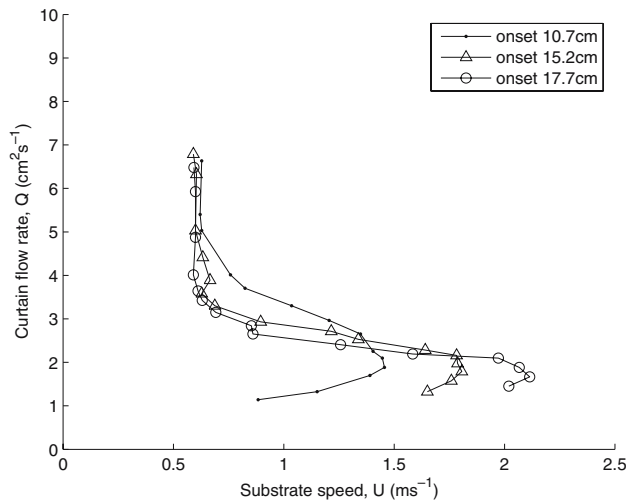
Fig. 2 Air entrainment curves for a 0.097 Pa s solution. The curtain heights are h = 10.7, 15.2 and 17.7 cm. The data points shown are for a purely horizontal examination, i.e. fixing Q and increasing U. $Re \in (1.29, 9.08)$, $We \in (2.74, 19.2)$, $(3.2, 22.9)$, $(3.52, 24.6)$, $Ca \in (0.91, 2.12)$, $(0.79, 2.63)$, $(0.82, 3.08)$

dent on h but U_i is not. This behaviour is consistent with previous observations of air entrainment (Blake et al. 1994; Blake et al. 1999; Yamamura et al. 1999). Once Q_i is reached, inertial effects are negligible and the onset of instability is determined by the viscous drag and surface tension forces alone. The hysteresis and vertical examinations for this fluid are not shown.

Figure 3a, b and c shows the examination of instability boundaries for a higher viscosity solution ($\mu = 0.181$ Pa s) at the same values of h. Figure 3a shows both onset and clearance data points for the horizontal examination represented by circles and stars, respectively, for a curtain height of 10.7 cm (103 μm < w < 414 μm). The discrepancies between these two data sets indicates a small hysteretic effect which, for Newtonian fluids is unique to the case where the surface is pre-wetted (with the exception of rough surfaces as demonstrated by Clarke 2002). In this figure, the vertical examination is also presented as shown by the vertical lines containing two or three data points. The lower-most data point is the clearance of air entrainment by increasing Q, the top data point is for the onset of air entrainment by further increase in Q and the intermediate point is for the clearance by decreasing Q. Thus the difference between the top and intermediate points is the hysteresis region in the vertical analysis. The coincidence of both the horizontal and vertical analyses for this regime of "regular" (termed "mode 1") assist has been previously reported by Marston et al. (2006b). Examples of mode 1 assist can also be seen in Blake et al. (2004) and Marston et al. (2006a).

On increasing the curtain height to 15.2 cm (87 μm < w < 347 μm), as shown in Fig. 3b, U_{max} could not be determined due to limitations of equipment in the range 2.7 cm² s⁻¹ < Q ≤ 3.8 cm² s⁻¹ and no instability could be detected across the entire range of speeds which could be produced by the equipment. The usual horizontal analysis (onset-clearance) data points are shown (where possible) along with the vertical analysis where, for $U > 1$ m s⁻¹, it is not possible to tell if the upper data point (onset by increasing Q) coincides with any critical speed from a horizontal analysis. The general shape of a curve joined by these points would indicate an extended stable region as suggested by Marston et al. (2006b).

This indicates that there is some critical impingement speed $u_c = \sqrt{2gh}$ (dependent only on h) at which the type of hydrodynamic assist switches to a more intense regime (termed "mode 2"), first postulated by Blake et al. (2004). This is clarified by further increasing h to 17.7 cm (80 μm < w < 322 μm) in Fig. 3c, where the effect is even more profound and new phenomena can be observed (termed "mode 3"). For $Q ≤ 2.2$ cm² s⁻¹ there is indeed intense hydrodynamic assist with rapidly increasing substrate speeds, as in Fig. 3(b). For 2.2 cm² s⁻¹ < Q ≤ 4.16 cm² s⁻¹, no air entrainment could be detected. For Q above this range, however, a noticeable "heel" forms which, as speed is increased, entrains air which becomes trapped within the heel and is visibly seen to recirculate, these data points are shown by diamonds. From this point, as speed is increased further, the heel becomes unstable and gross failure occurs. However, if the speed is increased up to the maximum wheel speed (2.3 m s⁻¹), the unstable heel formation can be cleared manually by means of a scraper blade placed just behind the curtain. This method of manual clearance, by removal of the air boundary layer, was first reported by Brown (1961) and has been reproduced in the patent literature as a means of maintaining successful coating. Once cleared, the contact line will remain stable, indicating that there is a large region where multiple states can occur. If U is subsequently reduced from this now stable configuration, a secondary critical speed becomes apparent—namely that at which instability recommences—indicated by triangles ("onset down" data points). This instability will remain until U is further reduced to beyond the boundary of "recirc + heel". The vertical examination here is also subject to hysteresis, but in general coincides with the "onset" and "onset down" data points.

The examinations presented in Figs. 2 and 3 for the three curtain heights show, for the first time, the qualitative change in behaviour, i.e. switch from mode
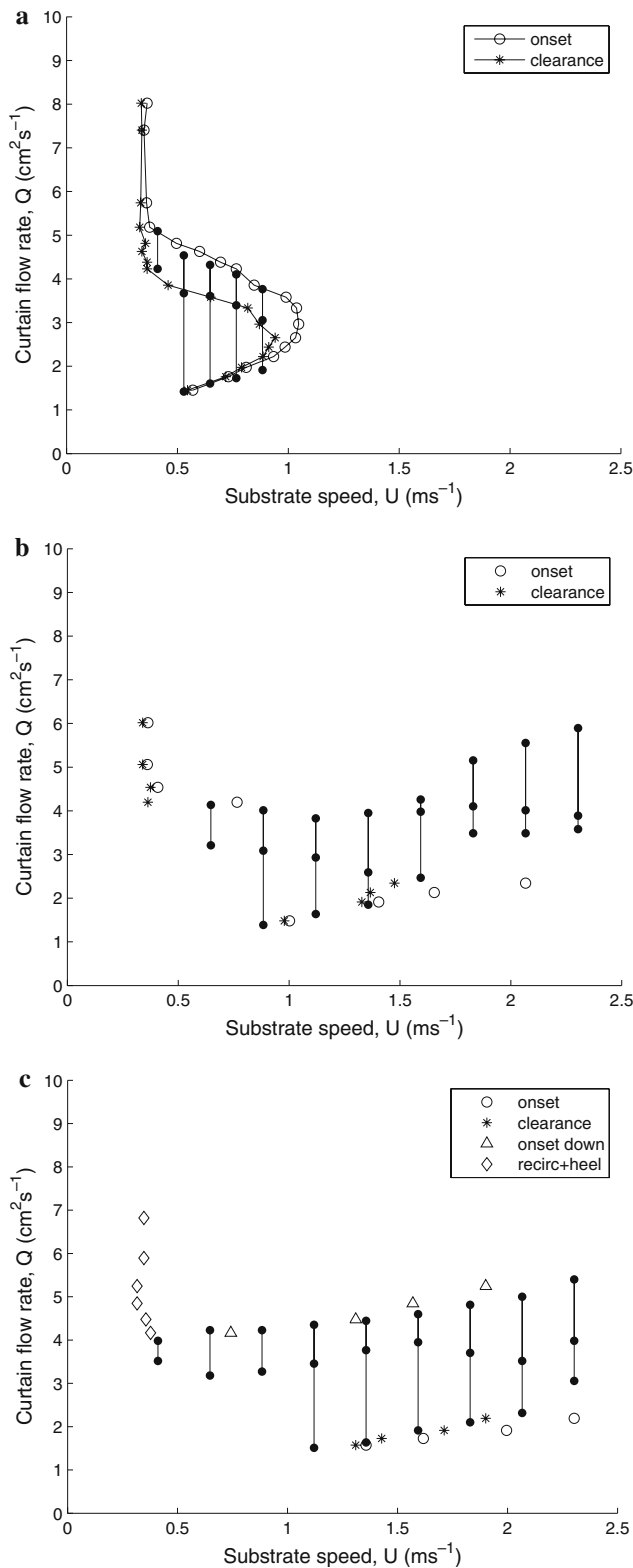
a

b

c

Fig. 3 Coating windows for a 0.181 Pa s glycerol solution form curtain heights of **a** 10.7 cm ($Re \in 0.7, 5.61$), $We \in (2.76, 22.1)$, $Ca \in (0.95, 2.85)$, **b** 15.2 cm ($Re \in 0.7, 4.21$), $We \in (3.29, 19.7)$, $Ca \in (0.98, 5.61)$ and **c** 17.7 cm ($Re \in 0.7, 4.91$), $We \in (3.54, 24.8)$, $Ca \in (0.86, 6.26)$. The three curtain heights identify three different regimes of hydrodynamic assist, now labeled as modes 1, 2 and 3, respectively. The data points in each graph constitute horizontal examinations whereas the *vertical lines with dots* show the vertical examination. The *lowermost dots* of the vertical analyses represent clearance of instability and the *intermediate dots* also represent clearance of instability by decreasing Q from the *uppermost dots*

and instability cannot be cleared, whereas to the right of the triangles, instability can be manually cleared and stability will persist. As such, the parameter space can be split into regions which are stable, subject to hysteresis, always unstable and metastable. A sketch of the Q–U parameter space broken into these regions is shown in Fig. 4.

To reinforce this conjecture, the same phenomenon is also seen in Fig. 5 with supporting images in Fig. 6. The curtain height $h = 17.7$ cm with $\mu = 0.213$ Pa s. The vertical and horizontal analyses provide excellent agreement, whilst the hysteresis in the vertical analysis appears to be becoming substantial. The images set around the plot represent both stable and unstable configurations, with the three images on the right all for identical parameters in sequence (top to bottom) of unstable, manual clearance and subsequent stable contact line.

From the above results on the pre-wetted surface and previously published results, it is possible to identify the crucial parameters for the qualitative switch in behaviour to occur. Clearly the viscosity and the impingement speed are the dominant parameters
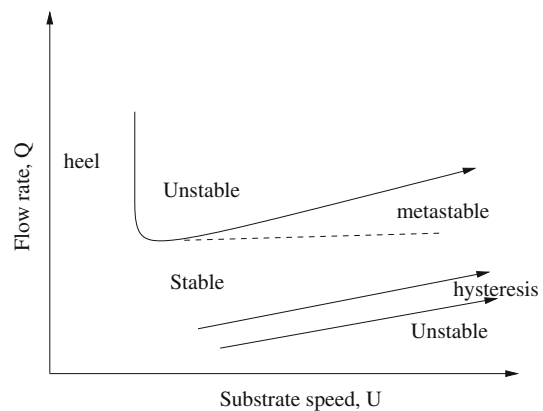

Fig. 4 Q–U parameter space identifying regions of differing stability for mode 3 assist. The *arrows* on the boundary lines indicate a possible continuation, not detected in these experiments

$1 \rightarrow$ mode $2 \rightarrow$ mode 3, for increasing both the viscosity and impingement speed.

It can be shown that the region to the right of the diamonds and above the triangles is always unstable
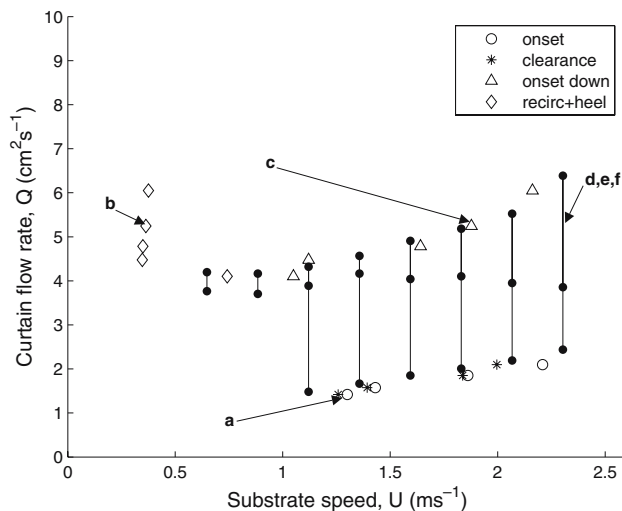
Fig. 5 Mode 3 type hydrodynamic assist for a 0.213 Pa s glycerol solution with horizontal and vertical analyses. The data points marked by *triangles* are for the onset of instability by decreasing *U*. The *arrows* mark the locations at which images **a–f** were taken, presented in Fig. 6. $Re \in (0.59, 3.58)$, $We \in (3.54, 21.2)$, $Ca \in (1.11, 7.34)$

in determining the degree of assist, as should be expected since the heel formation and air entrainment (instability) will depend on both inertia and viscous

drag forces (note that whilst the effect of surface tension is also likely to be significant, it cannot be examined as thoroughly due to the range of available fluids).

By identifying the three modes of assist in Fig. 3a, b and c as modes 1, 2 and 3, respectively, Table 1 presents data examining viscosities and curtain heights/impingement speeds at which the type of hydrodynamic assist switches to a more intense mode (note that all liquids here are Newtonian in nature).

With reference to Figs. 3 and 4 in Blake et al. (2004), it can be deduced that the switch in mode of assist is qualitatively similar to that reported here, only that in the current work the curtain heights are lower, due to a combined effect of the lower viscosity and the effect of the residual film on the substrate.

For the pre-wet surface, an increase in impingement speed from 1.45 to 1.73 m s^{-1}, for $\mu = 0.181$ Pa s leads to a switch from mode 1 to 2 and a further increase to 1.86 m s^{-1} switches to mode 3. Clearly the critical speed could lie somewhere between the values tested here, but this will depend upon viscosity and hence to determine the exact value at each viscosity would be difficult. For the data of Blake et al. (2004) onto dry tape, the switches are qualitatively similar, but occur at higher impingement speeds.

Fig. 6 Images corresponding to those indicated on Fig. 5: **a** "vvv"-type air entrainment, **b** heel with recirculation, **c** gross failure onset from decreasing *U*, **d** gross failure at max. wheel speed by increasing *U*, **e** manual clearance of unstable heel at max. wheel speed and **f** subsequent stable contact line. Images **d**, **e** and **f** are for identical *Q* and *U*
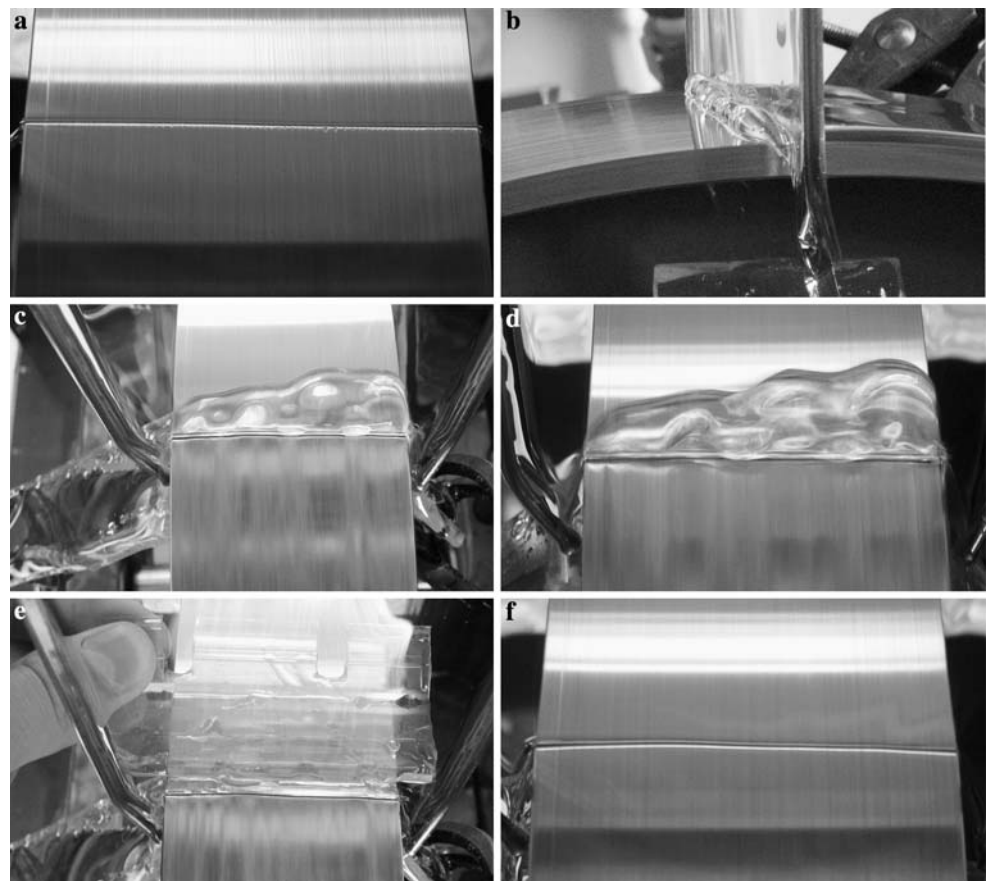
Table 1 Comparison of available data onto dry and pre-wet surfaces showing a switch to a more intense mode of hydrodynamic assist by increases in either impingement speed or liquid viscosity

Data	μ (Pa s)	h (cm)	u_c (m s^{-1})	Assist mode switch
Marston et al. (2006b)	0.706 $\rightarrow$ 0.878	8.5	1.29	1 $\rightarrow$ 2
Marston et al. (2006b)	0.462	8.5 $\rightarrow$ 9.5	1.29 $\rightarrow$ 1.36	1 $\rightarrow$ 2
Fig. 2	0.097	10.7, 15.2, 17.7	1.45, 1.73, 1.86	1 (no switch)
Fig. 3	0.181	10.7 $\rightarrow$ 15.2	1.45 $\rightarrow$ 1.73	1 $\rightarrow$ 2
Fig. 3	0.181	15.2 $\rightarrow$ 17.7	1.73 $\rightarrow$ 1.86	2 $\rightarrow$ 3
Blake et al. (2004)	0.32	10.2 $\rightarrow$ 17.8	1.41 $\rightarrow$ 1.87	1 $\rightarrow$ 2
Blake et al. (2004)	0.32	17.8 $\rightarrow$ 20.1	1.87 $\rightarrow$ 1.99	2 $\rightarrow$ 3

The switches in mode of assist clearly favour a high liquid viscosity and impingement speed and occur at lower values of both parameters when the surface is pre-wet, due to the pre-existing film "lubricating" the curtain's impingement thus increasing potential for hydrodynamic assist to occur.

4 Conclusions

Three modes of hydrodynamic assist have been observed and studied in a curtain coating geometry using a pre-wetted surface. By increasing either the viscosity or impingement speed, a more intense mode of assist can occur. For impingement speeds $u_c \geq 1.86$ m s^{-1} and viscosity $\mu \geq 0.181$ Pa s, very high coating speeds can be expected, if the instability boundary is approached entirely through the stable domain. When these conditions are met, one can split the parameter space into regions of absolute stability, instability, metastability and regions subject to hysteresis.

The qualitative switch in mode of hydrodynamic assist demonstrated here was obtained by increasing curtain heights over a range of flow rates. Throughout the range of flow rates tested, the curtain widths range from 80 μm $< w <$ 322 μm for $h = 17.7$ cm, 87 μm $< w <$ 347 μm for $h = 15.2$ cm and 103 μm $< w <$ 414 μm for $h = 10.7$ cm and the pressure loads $\rho u_c^2 \sim$ 4.4, 3.8 and 2.6 kPa, respectively. It is likely to be these increments in pressure load suppressing air entrainment which leads to a more intense mode of assist.

Blake et al. (2004) suggest that the smaller curtain widths may be responsible for these more intense modes of assist since the lengthscale of the flow is approaching the wetting lengthscale, thus maximising the potential for assist. However, this now seems unlikely given such a dramatic change in behaviour for such small changes in curtain widths. In light of this, more data is needed, in particularly for dry substrates and for fluids of different surface tension to examine the phenomenon reported here more thoroughly and make quantitative predictions about the occurrence of such a switch in behaviour.

References

Benkreira H (2004) The effect of substrate roughness on air entrainment in dip coating. Chem Eng Sci 59:2745–2751

Blake TD, Clarke A, Ruschak KJ (1994) Hydrodynamic assist of dynamic wetting. AIChE J 40(2):229–242

Blake TD, Bracke M, Shikhmurzaev YD (1999) Experimental evidence of nonlocal hydrodynamic influence on the dynamic contact angle. Phys Fluids 11:1995–2007

Blake TD, Dobson RA, Ruschak KJ (2004) Wetting at high capillary numbers. J Colloid Interface Sci 279:198–205

Brown DR (1961) A study of the behaviour of a thin sheet of moving liquid. J Fluid Mech 10:297–305

Clarke A (2002) Coating on a rough surface. AIChE J 48:2149–2156

Marston JO, Simmons MJH, Decent SP, Kirk SP (2006a) Influence of the flow field in curtain coating onto a pre-wet substrate. Phys Fluids 18:112102

Marston JO, Decent SP, Simmons MJH (2006b) Hysteresis and non-uniqueness in the speed of onset of instability in curtain coating. J Fluid Mech 569:349–363

Yamamura M, Suematsu S, Toshihisa K, Adachi K (1999) Experimental investigation of air entrainment in a vertical liquid jet flowing down onto a rotating roll. Chem Eng Sci 55:931–942

Yamamura M, Matsunaga A, Matawari Y, Adachi K, Kage H (2006) Particle-assisted dynamic wetting in a suspension liquid jet impinged onto a moving substrate at different flow rates. Chem Eng Sci 61(16):5421–5426